

## Broadband dielectric spectroscopy on glass-forming propylene carbonate

U. Schneider, P. Lunkenheimer, R. Brand, and A. Loidl

*Experimentalphysik V, Universität Augsburg, D-86135 Augsburg, Germany*

(Received 10 December 1998)

Dielectric spectroscopy covering more than 18 decades of frequency has been performed on propylene carbonate in its liquid and supercooled-liquid state. Using quasioptic submillimeter and far-infrared spectroscopy, the dielectric response was investigated up to frequencies well into the microscopic regime. We discuss the  $\alpha$  process whose characteristic time scale is observed over 14 decades of frequency and the excess wing showing up at frequencies some three decades above the peak frequency. Special attention is given to the high-frequency response of the dielectric loss in the crossover regime between  $\alpha$  peak and boson peak. Similar to our previous results in other glass-forming materials, we find evidence for additional processes in the crossover regime. However, significant differences concerning the spectral form at high frequencies are found. We compare our results to the susceptibilities obtained from light scattering and to the predictions of various models of the glass transition. [S1063-651X(99)06406-5]

PACS number(s): 64.70.Pf, 77.22.-d, 78.30.Ly

### I. INTRODUCTION

Despite a long history of research on the glass transition [1], this phenomenon is still commonly regarded as an unresolved problem. In recent years a variety of new theoretical and phenomenological approaches of the glass transition (e.g., [2–9]) stimulated new experimental investigations of the dynamic response of glass-forming liquids (see, e.g., [10–20]). Here dielectric spectroscopy has played an important role, mainly due to the broad dynamic range accessible with this method (e.g., [8,9,16–22]). Spectra of the dielectric loss  $\epsilon''$  show a variety of features, the microscopic origin of most of them being still controversially discussed. Most prominent is the  $\alpha$  peak associated with the well known  $\alpha$  or structural-relaxation process. The comparison of the non-trivial temperature dependence of the  $\alpha$ -relaxation time with theoretical predictions states an important test for any model of the glass transition. Some decades above the  $\alpha$ -peak frequency  $\nu_p$ , an excess wing (also called “high-frequency wing” or “tail”) shows up as a high-frequency excess contribution to the power law  $\nu^{-\beta}$ , commonly found at  $\nu > \nu_p$ . This excess wing was already noted in the early work of Davidson and Cole [23]. It seems to be a universal feature of glass-forming liquids (at least if a  $\beta$  relaxation is absent) as can be deduced from the scaling behavior found by Nagel and co-workers [8]. Based on this universal scaling of  $\alpha$  relaxation and excess wing, Nagel and co-workers [9] proposed a divergence of the static susceptibility which essentially implies a constant loss behavior at high frequencies and low temperatures as has early been predicted by Wong and Angell [24]. The interest in even higher frequencies, in the GHz-THz region, was mainly stimulated by the mode coupling theory (MCT) [2–4], which explains the glass transition in terms of a dynamic phase transition at a critical temperature  $T_c$  significantly above the glass temperature  $T_g$ . From neutron- and light-scattering experiments it is well known that in the THz region the so-called boson peak shows up in the imaginary part of the susceptibility of glass-forming liquids. For the transition region between the  $\alpha$  process and boson peak, MCT predicts an additional contribu-

tion, now commonly termed fast  $\beta$  relaxation. But also other models predict fast processes, the most prominent being the coupling model by Ngai and co-workers [5]. This transition region was mainly investigated by neutron and light scattering and indeed indications for additional fast processes were found [11,12,14,15]. The scattering results were described within the framework of MCT and partly good agreement with the theoretical results was obtained. However, the applicability of the MCT for glass-forming liquids, especially at low temperatures near  $T_g$ , is still a matter of controversy. Dielectric data were scarce in the relevant high-frequency region as for classical dielectric methods the region above GHz is not accessible. Only recently, our group was able to obtain continuous dielectric spectra on glass-forming liquids extending well into the submillimeter wavelength region [18–20,25–27]. The existence of a broad minimum in  $\epsilon''(\nu)$  was found which cannot be explained by a simple crossover from the structural ( $\alpha$ ) relaxation to the far-infrared (FIR) vibrational response. Similar to the scattering results, clear indications for additional fast processes prevailing in this transition region were found. For glass-forming glycerol, by combining classical dielectric spectroscopy, coaxial transmission, and quasioptic submillimeter and far-infrared techniques, spectra covering 18 decades of frequency and extending well into the THz range were obtained [27]. This allowed for the observation of the complete dynamic response including the boson peak. In addition, dielectric spectra up to 380 GHz were obtained in  $[\text{Ca}(\text{NO}_3)_2]_{0.4}[\text{KNO}_3]_{0.6}$  (CKN) and  $[\text{Ca}(\text{NO}_3)_2]_{0.4}[\text{RbNO}_3]_{0.6}$  (CRN) [19,20,25]. Both are ionically conducting, molten-salt glass formers with relatively high fragility [28,29],  $m \approx 90$  [30]. In contrast, glycerol is a rather strong hydrogen-bonded glass former with a fragility parameter of  $m \approx 53$  [31]. In many respects, especially concerning the high-frequency response near the boson peak and the agreement of the dielectric data with MCT predictions and with the scattering results, glycerol and the molten salts behave qualitatively different. In order to clarify the origin of these differences and in light of the dependence of the boson peak contribution on fragility [32], it seemed of interest to investigate a fragile but molecular

glass former. For this purpose we have chosen propylene carbonate (PC), which like glycerol is a molecular glass former, but can be characterized as a fragile ( $m \approx 104$  [31]) van der Waals liquid. Preliminary results on PC in a somewhat restricted frequency range have been published earlier [19,25,26]. In the present paper we present extended results covering the complete dynamic range including the boson peak. We address all features seen in the dielectric spectra, i.e., the  $\alpha$  response, the excess wing, the fast  $\beta$ -relaxation region, and the boson peak. The results are compared with a variety of theoretical predictions and with the findings from other experimental methods.

## II. EXPERIMENTAL DETAILS

The measurements presented in this paper have been performed using a variety of different techniques to cover nearly 20 decades in frequency. The lowest frequencies ( $10 \mu\text{Hz} \leq \nu \leq 1 \text{ kHz}$ ) were investigated in the time domain using a spectrometer that is based on a design described by Mopsik [33]. The complex dielectric constant was calculated from the measured response function via a Fourier transformation. The autobalance bridges HP4284 and HP4285 were used in the range  $20 \text{ Hz} \leq \nu \leq 20 \text{ MHz}$ . For the radio-frequency and microwave range ( $1 \text{ MHz} \leq \nu \leq 10 \text{ GHz}$ ) a reflectometric technique was employed [34] using the HP4191 and HP4291 impedance analyzers and the HP8510 network analyzer. In addition, at frequencies  $100 \text{ MHz} \leq \nu \leq 30 \text{ GHz}$ , data were taken in transmission with the HP8510 network analyzer using 7 mm coaxial lines of various lengths (between 10 and 300 mm) filled with the sample material. Closed-cycle refrigerators,  $\text{N}_2$ , and He cryostats have been used to cover the relevant temperature ranges.

At frequencies  $40 \text{ GHz} \leq \nu \leq 1.2 \text{ THz}$  a quasioptical submillimeter spectrometer was used with an experimental arrangement similar to a Mach-Zehnder interferometer [35]. This setup allows for measuring the frequency dependence of both the transmission and the phase shift of a monochromatic electromagnetic beam through the sample. The frequency range up to 1.2 THz is covered continuously by 10 tunable narrow-band backward-wave oscillators (BWOs). The signal was detected by a Golay cell or a pumped He bolometer and amplified using lock-in techniques. The liquid was put in specially designed cells made of polished stainless steel with thin plane-parallel quartz windows; depending on the range of frequency and temperature the thickness of the sample cell was between 1 mm and 30 mm. The sample cell was placed in a home-made cryostat and cooled by a continuous flow of nitrogen gas. The data were analyzed using optical formulas for multilayer interference [36] with the known thickness and optical parameters of the windows in order to get the real and imaginary part of the dielectric constant of the sample as a function of frequency at various temperatures. At higher frequencies the samples were investigated with a Fourier-transform infrared spectrometer covering a regime from 450 GHz to 10 THz. This setup allows the measurement of the transmission or reflection only, whereas the phase shift caused by the sample cannot be determined.

To cover the complete frequency range, a single  $\epsilon''(\nu)$  curve at a given temperature is superimposed using results

from the various setups. The time-domain results are obtained in arbitrary units and scaled by one factor to match the autobalance bridge results. For the measurements at  $1 \text{ GHz} \leq \nu \leq 40 \text{ GHz}$  there are some uncertainties of the absolute values originating from an ill-defined geometry of the samples or parasitic elements. These results have been partly shifted by one scaling factor per measurement series which led to a good match at both the low- and the high-frequency side. Typically, shifting factors of less than 20% had to be applied to obtain smooth curves. The submillimeter-frequency results and, at losses  $\epsilon'' \geq 1$ , also the coaxial transmission measurements provide excellent absolute values of  $\epsilon'$  and  $\epsilon''$ . The values for  $\epsilon''$  from the infrared measurements were calculated consistently with the Kramers-Kronig relation assuming a reasonable behavior of the dielectric constant  $\epsilon'$  which is almost constant in this frequency regime. In this latter case, the error bars for  $\epsilon''$  were estimated by a variation of the assumed  $\epsilon'$  behavior.

As sample material, propylene carbonate ( $T_g = 159 \text{ K}$  [37],  $T_m = 218 \text{ K}$ ) with a purity of 99.7%, was used. To avoid crystallization, polished sample holders had to be used in the various experiments. However, occasional crystallization, mainly at temperatures around 180 K, could not be avoided completely. Therefore, some measurements were performed after heating up to  $T_m$  and direct cooling to each measurement temperature with relatively fast cooling rates (1 K/min).

## III. RESULTS

### A. $\alpha$ relaxation and excess wing

Figures 1 and 2 show  $\epsilon'(\nu)$  and  $\epsilon''(\nu)$  for various temperatures in the whole accessible frequency range.  $\epsilon''(\nu)$  (Fig. 2) exhibits the typical asymmetrically shaped  $\alpha$ -relaxation peaks shifting through the frequency window with temperature. They are accompanied by relaxation steps in  $\epsilon'(\nu)$  as seen in Fig. 1. In most respects the data agree well with the results of earlier dielectric investigations of PC [37–45] which were restricted to smaller frequency and temperature ranges. However, some differences show up in the absolute values (see below). The solid lines in Figs. 1 and 2 are fits of the  $\alpha$ -relaxation region with the empirical Cole-Davidson function [23],  $\epsilon^* = \epsilon_\infty + (\epsilon_s - \epsilon_\infty) / (1 + i2\pi\nu\tau_{\text{CD}})^{\beta_{\text{CD}}}$ , performed simultaneously for real and imaginary part.  $\epsilon_s$  and  $\epsilon_\infty$  denote the low- and high-frequency limit of the dielectric constant, respectively. A good fit of the peak region was achieved. Very close to the maximum the loss curves can also be described by the Fourier transform of the Kohlrausch-Williams-Watts (KWW) function [46],  $\Phi = \Phi_0 \exp[-(t/\tau_{\text{KWW}})^{\beta_{\text{KWW}}}]$  (dotted lines, shown for 173 K only). For all temperatures investigated the KWW fit is of lower quality than the CD fit. This can be ascribed to the fact that there is a significant difference of CD and KWW response concerning the loss-peak region. For the KWW response the curvature near the peak is retained somewhat further above the peak frequency and a power law  $\epsilon'' \sim \nu^{-\beta_{\text{KWW}}}$  is approached at significantly higher frequencies only. Therefore, in most cases the exponent  $\beta_{\text{KWW}}$  obtained from the KWW fits differs significantly from the power-law exponent  $\beta$  actually observed for  $\nu > \nu_p$ . In contrast, for the CD fits  $\beta_{\text{CD}} = \beta$  is found. Despite the fact that

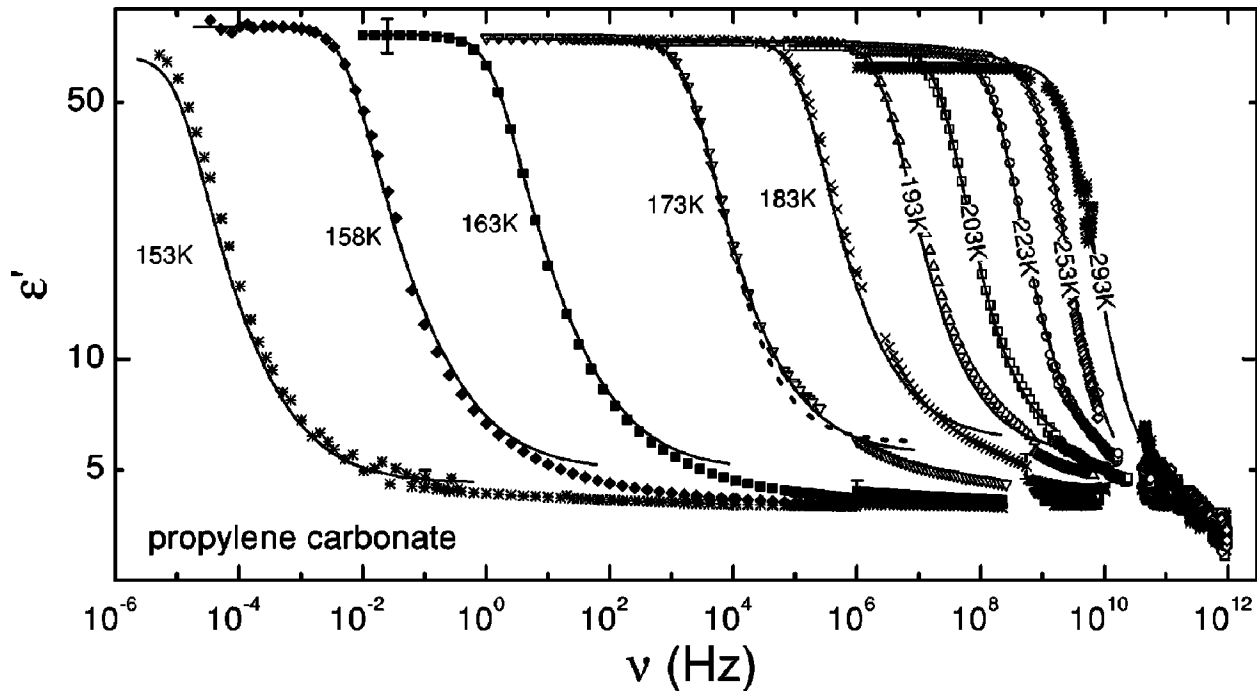


FIG. 1. Frequency dependence of the dielectric constant in PC at various temperatures. The solid lines are fits with the CD function performed simultaneously on  $\epsilon''$ . The dotted line is a fit with the Fourier transform of the KWW function.

the KWW function is more widely used nowadays, in the authors' experience dielectric loss data in glass-forming materials are often described much better by the CD function [22,26,27,47]. The inset of Fig. 2 shows the temperature dependence of the frequency  $\nu_\tau = 1/(2\pi\langle\tau\rangle)$  which is virtually identical to the peak frequency  $\nu_p$ . Here  $\langle\tau\rangle$  denotes

the mean relaxation time [48] calculated from  $\langle\tau\rangle_{CD} = \beta_{CD}\tau_{CD}$  for the CD function and  $\langle\tau\rangle_{KWW} = \tau_{KWW}/\beta_{KWW} \times \Gamma(1/\beta_{KWW})$  ( $\Gamma$  denoting the Gamma function) for the KWW function. The results from the CD (circles) and the KWW fits (pluses) agree perfectly well and are in accord with previously published data [37,38,41–43,49].  $\nu_\tau(T)$

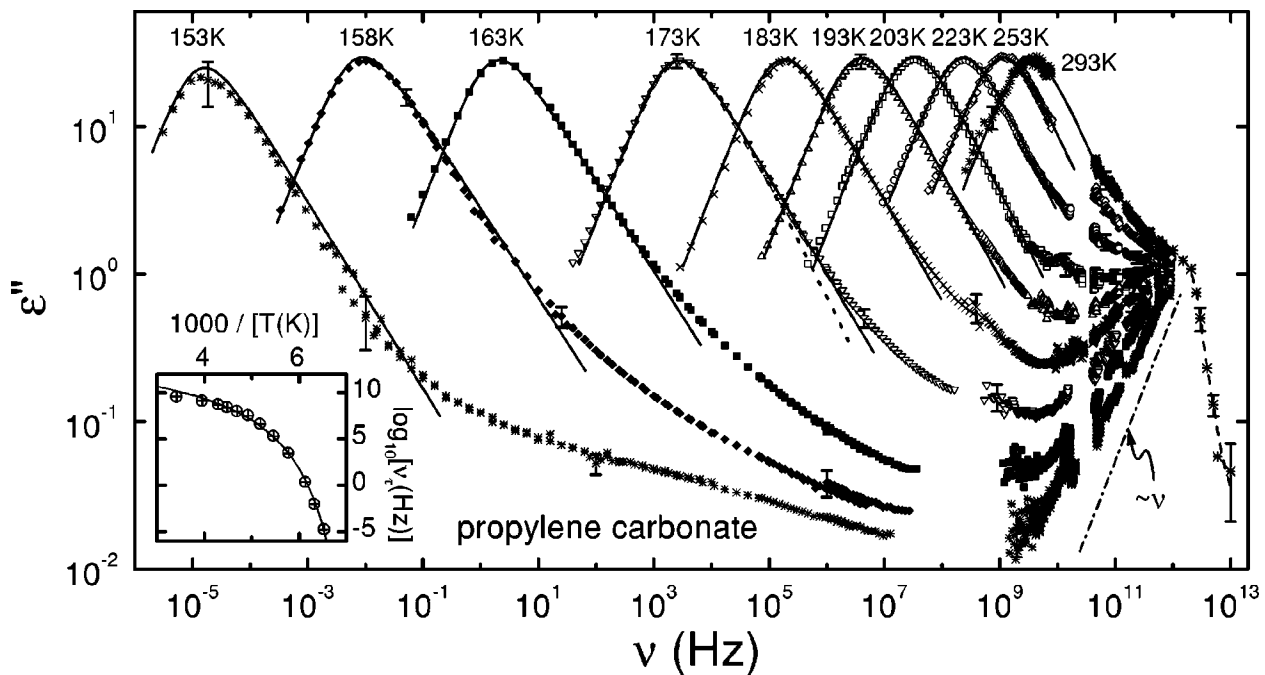


FIG. 2. Frequency dependence of the dielectric loss in propylene carbonate at various temperatures. The solid lines are fits with the CD function, the dotted line is a fit with the Fourier transform of the KWW law, both performed simultaneously on  $\epsilon''$ . The dash-dotted line indicates a linear increase. The FIR results have been connected by a dashed line to guide the eye. The inset shows  $\nu_\tau = 1/(2\pi\langle\tau\rangle)$  as resulting from the CD (circles) and KWW fits (pluses) in an Arrhenius representation. The line is a fit using the VFT expression, Eq. (1), with  $T_{VF} = 132$  K,  $D = 6.6$ , and  $\nu_0 = 3.2 \times 10^{12}$  Hz.

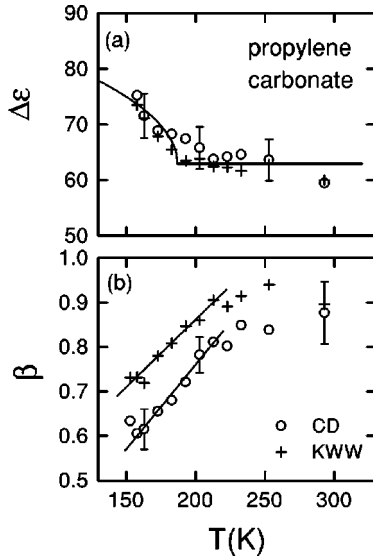


FIG. 3. Relaxation strength  $\Delta\epsilon$  (a) and width parameter  $\beta$  (b) as obtained from simultaneous fits of  $\epsilon'(\nu)$  and  $\epsilon''(\nu)$  using the CD function and the Fourier transform of the KWW function. The solid line in (a) has been calculated using the MCT prediction (see text). The solid lines in (b) indicate a linear increase.

shows the well known deviations from thermally activated behavior, typical for fragile glass formers. It can be parametrized using the Vogel-Fulcher-Tammann (VFT) equation [50] (line in the inset of Fig. 2; see Sec. IV A).

In Fig. 3(a) the relaxation strengths  $\Delta\epsilon = \epsilon_s - \epsilon_\infty$  obtained from the CD and KWW fits are shown. One has to be aware that  $\Delta\epsilon$  resulting from the fits is somewhat smaller than  $\Delta\epsilon$  read off from the  $\epsilon'(\nu)$  data of Fig. 1. As seen in Fig. 1, the fits overestimate  $\epsilon_\infty$  because there is an additional decrease of  $\epsilon'(\nu)$  corresponding to the excess wing contribution (see below) which is not taken into account by the CD fits. Consequently  $\Delta\epsilon$  shown in Fig. 3(a) presents the relaxation strength of the  $\alpha$  process alone, without the excess wing contribution.  $\Delta\epsilon$  decreases monotonically with temperature which is in accord with previous reports [37,39,43]. However, the decrease found in the present work is somewhat less steep than reported earlier. Unfortunately, in [43] where a rather broad temperature and frequency range was investigated, no absolute values of  $\Delta\epsilon$  were reported. The results from the high-frequency measurements of Payne and Theodorou [39] are compatible with our data at  $T > 273$  K except for their lowest temperature (195 K), where a much higher value ( $\Delta\epsilon \approx 86$ ) was found. However, the relaxation time at 195 K reported by these authors deviates by more than one decade from that found in the present and other works [43,49], which sheds some doubt upon the significance of the results at this temperature. Also from the results of Huck *et al.* [41] and Angell *et al.* [37] near 170 K a much higher magnitude of  $\Delta\epsilon$  ( $> 100$ ) than determined here can be read off. The determination of the absolute values of  $\Delta\epsilon$  is a difficult task as it depends on the shifting factors necessary to match results from different experimental setups and on the subtraction of possible stray capacitances inherent to some methods. We believe that due to the broad overlap of the frequency ranges of the various devices used in the present work, the reproducibility of results with different

sample holders, and the simultaneous fitting of  $\epsilon'(\nu)$  and  $\epsilon''(\nu)$ , Fig. 3(a) gives a good estimate of the absolute value of  $\Delta\epsilon$ .

Figure 3(b) shows the width parameter obtained from both fitting procedures. Both  $\beta_{CD}$  and  $\beta_{KWW}$  increase nearly linearly with temperature up to about 200 K. Above this temperature a tendency to saturate at a value below unity is observed. This is in contrast to [43], where  $\beta_{CD}(T)$  was reported to saturate at unity for high temperatures. This discrepancy may be due to the smaller frequency range available in [43], which for high temperatures leads to a restriction of the data at the high-frequency side of the loss peaks, which is essential for the determination of  $\beta_{CD}$ . Unfortunately, no  $\epsilon''(\nu)$  data of PC are shown in [43].

At frequencies about two to three decades above  $\nu_p$ , deviations of  $\epsilon''(\nu)$  from the CD fits show up. For low temperatures these deviations can be described as a second power law,  $\epsilon'' \sim \nu^{-b}$  with  $b < \beta$ , in addition to the power law  $\epsilon'' \sim \nu^{-\beta}$  constituting the high-frequency flank of the  $\alpha$  peak. The exponent  $b$  decreases with decreasing temperature as found previously for PC and other glass-forming materials [45]. The excess wing is accompanied by a decrease in  $\epsilon'(\nu)$  as mentioned above. It shows up as a somewhat smoother rounding of the  $\epsilon'(\nu)$  curves (compared, e.g., to the CD behavior) when approaching  $\epsilon_\infty$  (Fig. 1). For  $T = 193$  K the exponent  $b$  has reached a value almost identical with  $\beta_{CD}$  (Fig. 2) and for 203 K the excess wing seems to have merged with the  $\alpha$  peak. For  $T \geq 203$  K the deviations of the experimental data from the CD fits are due to the fast dynamic processes described in the following section.

## B. Fast dynamics

At high frequencies, succeeding the excess wing for low and the  $\alpha$  peak for high temperatures,  $\epsilon''(\nu)$  exhibits a smooth transition into a shallow minimum. Such a minimum was earlier observed in glycerol [18,19,26,27], Salol [19,26], the molten salts CKN [16,17,19,20,25], and CRN [20], and the plastic crystals cyclo-octanol [47,51] and ortho-carborane [51]. With increasing temperature, the amplitude  $\epsilon_{\min}$  and frequency position  $\nu_{\min}$  of the minimum increases. For room temperature the measurements have been extended into the FIR region. Here no minimum is observed, but a shoulder shows up near 1 THz. This shoulder is indicative of the so-called boson peak or microscopic peak known mainly from neutron- and light-scattering measurements [11,12,14,15]. Indeed, for PC the boson peak, determined from light-scattering measurements [15], is located just above 1 THz. As the peak frequency and amplitude is only weakly temperature dependent, it becomes obvious that the high-frequency flank of the  $\epsilon''(\nu)$  minimum is identical to the low-frequency flank of the boson peak. The frequency dependence in this region can be approximately described by a power law  $\epsilon'' \sim \nu^a$ . The exponent  $a$  increases with decreasing temperature and seems to approach a linear behavior as indicated by the dash-dotted line in Fig. 2. In  $\epsilon'(\nu)$  for these frequencies the onset of a relaxation step corresponding to the boson peak can be seen (Fig. 1).

In Fig. 4 we compare  $\epsilon''(\nu)$  with  $\chi''(\nu)$  calculated from the light-scattering results on PC [15]. As the light-scattering results give no information on the absolute values of  $\epsilon''$ , the

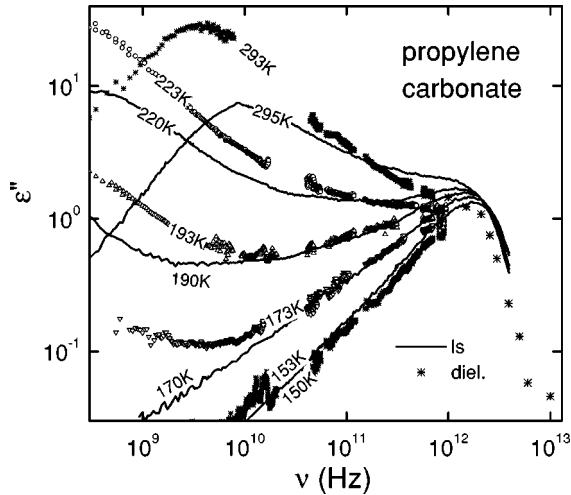


FIG. 4. Frequency dependence of the dielectric loss in propylene carbonate compared to the susceptibility as calculated from the light scattering results (from [15]). The light-scattering data sets have been vertically shifted to give a comparable intensity of the boson peak.

datasets have been scaled to yield a comparable height of the boson peak. While the dielectric results in PC are qualitatively similar to the light-scattering results (succession of  $\alpha$  peak, minimum, and boson peak), quantitative differences show up: The  $\alpha$  peak is located at a significantly lower frequency and the ratio of the amplitudes of the  $\alpha$  and the boson peak is higher for the dielectric measurements. The latter behavior was also found in our experiments on glycerol [26,27] and Salol [26], and in molecular-dynamics simulations of ortho-terphenyl [52] and of a system of rigid diatomic molecules [53]. The results from a very recent neutron-scattering study of PC [54] indicate an even smaller ratio of the  $\alpha$ - and the boson-peak amplitude than for light scattering. Clearly the position of the minimum differs between the different methods, also in accord with results on other systems [26,27,53]. In contrast, the increase towards the boson peak exhibits almost identical power laws for the dielectric and light-scattering measurements.

#### IV. DISCUSSION

##### A. $\alpha$ relaxation

The most significant result of an analysis of the  $\alpha$ -relaxation process is the temperature dependence of the  $\alpha$ -relaxation time which is compared to various predictions in Fig. 5. Figure 5(a) shows the same fit with the VFT equation [50],

$$\nu_{\tau} = \nu_0 \exp\left(\frac{-DT_{VF}}{T - T_{VF}}\right) \quad (1)$$

as in the inset of Fig. 2. A VFT temperature  $T_{VF} = 132$  K and a strength parameter  $D = 6.6$  were determined, the latter characterizing PC as a fragile glass former [28]. While the VFT equation is primarily an empirical description, a theoretical foundation was given in various models, e.g., the Adam-Gibbs theory [55] or the free volume theory [56].

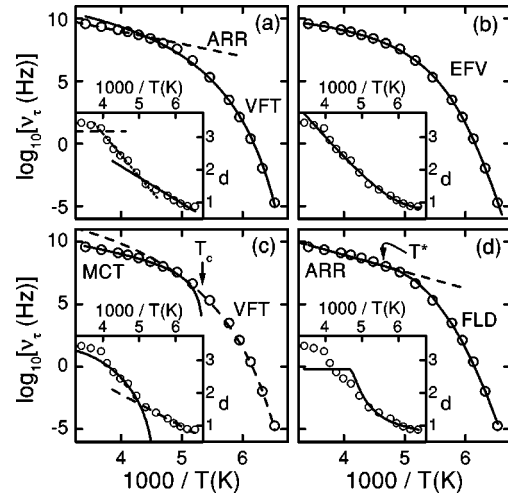


FIG. 5. Temperature dependence of  $\nu_{\tau} = 1/(2\pi\langle\tau\rangle_{CD})$  as determined from simultaneous CD fits of  $\varepsilon'(\nu)$  and  $\varepsilon''(\nu)$  in Arrhenius representation. (a) Solid line: fit with VFT behavior [Eq. (1),  $\nu_0 = 3.2 \times 10^{12}$  Hz,  $D = 6.6$ ,  $T_{VF} = 132$  K]; dashed line: Arrhenius behavior ( $\nu_0 = 9.0 \times 10^{12}$  Hz,  $E = 2290$  K). (b) Solid line: fit with EFV theory [Eq. (2),  $A = 10.7$ ,  $B = 309$  K,  $C = 4.82$  K,  $T_0 = 162$  K]. (c) Solid line: fit with MCT [Eq. (3),  $T_c = 187$  K,  $\gamma = 2.72$ ,  $c = 12900$ ].  $T_c$  and  $\gamma$  were fixed at the values determined from the evaluation of the  $\varepsilon''(\nu)$  minimum. Dashed line: fit with VFT behavior for  $T < 200$  K [Eq. (1),  $\nu_0 = 4.9 \times 10^{13}$  Hz,  $D = 8.4$ ,  $T_{VF} = 128$  K]. (d) Solid line: fit with FLD theory [Eq. (4),  $T^* = 215$  K,  $\nu_{\infty} = 2.03 \times 10^{14}$  Hz,  $E_{\infty} = 3090$  K,  $F = 457$ ]; dashed line: high-temperature asymptotic Arrhenius behavior. The insets in (a)–(d) show plots of  $d := [-d(\log_{10} \nu_p)/d(1/T)]^{-1/2}$  as suggested by Stickel *et al.* [58]. The lines are calculated with the same parameters as the lines in the corresponding main frames. The additional dotted line in the inset of (a) suggests a second VFT law above 200 K.

In Fig. 5(a) it becomes obvious that, above a crossover temperature  $T_A \approx 230$  K, deviations from VFT behavior show up, similar to those seen in earlier work [37,43,49]. In [37] and [43] a transition to thermally activated behavior was suggested as demonstrated by the dashed line in Fig. 5(a).  $T_A$  was interpreted [37] as temperature below which the potential energy landscape becomes important. However, one has to state that also alternative descriptions are possible, e.g., using VFT behavior at high and a thermally activated behavior at low temperatures or a combination of VFT functions [57]. In addition, Stickel *et al.* [49] performed an analysis of relaxation-time data on PC extending to temperatures above room temperature using a temperature-derivative method [58]. Here  $d := [-d(\log_{10} \nu_p)/d(1/T)]^{-1/2}$  is plotted versus  $1/T$ , which leads to a linear behavior for the VFT law and a constant for the Arrhenius law. This “Stickel plot” is shown in the inset of Fig. 5(a). The solid and the dashed lines are the transferred VFT and Arrhenius curves shown in the main frame. In this representation, deviations only weakly seen in the main frame become more pronounced. Near 200 K, a change of slope shows up which suggests a transition to a second VFT law above about 200 K as indicated by the dotted line. A very similar behavior was found by Stickel *et al.* [49]. The suggested Arrhenius behavior above about 230 K [main frame of Fig. 5(a)] seems not to be supported by the Stickel plot, but at least a tendency of  $d(T)$  to saturate at

high temperatures is seen. Stickel *et al.* [49] reported a transition to thermally activated behavior at a higher temperature of about 300 K. Overall, as demonstrated in Fig. 5(a), the three-parameter VFT function is not able to describe the data in the whole temperature range and a crossover to a different behavior has to be assumed to overcome this difficulty.

A four-parameter function for the description of  $\nu_\tau(T)$  is the outcome of the extended free volume (EFV) theory [59]. In the EFV theory the supercooled liquid is assumed to be divided into liquidlike and solidlike regions. At a temperature  $T_0$  a transition from percolating (fluid) to isolated liquidlike regions (solid glass state) occurs. By addressing the entropy of the glass-forming system and making use of percolation theory, the following result for  $\nu_\tau(T)$  was obtained:

$$\log_{10}(\nu_\tau) = -A - \frac{B}{T - T_0 + [(T - T_0)^2 + CT]^{1/2}}. \quad (2)$$

Good fits with Eq. (2) for a variety of glass formers were reported [12,59]. Figure 5(b) shows a fit of  $\nu_\tau(T)$  of PC with Eq. (2) and  $T_0 = 162$  K. Indeed, the EFV theory gives a very good description of the present data and  $T_0$  is almost identical to the calorimetric  $T_g \approx 159$  K [37]. Also in the Stickel plot, data and fit agree reasonably well.

While the VFT and EFV predictions lead to critical temperatures near or below  $T_g$ , the  $T_c$  of MCT is predicted to be located well above  $T_g$ . The simplest version of MCT, the idealized MCT [2,3], predicts a critical behavior of the  $\alpha$ -relaxation time scale,

$$\nu_\tau \sim (T - T_c)^\gamma, \quad (3)$$

with a critical exponent  $\gamma$  that is determined by  $\gamma = 1/(2a) + 1/(2b)$ . Here  $a$  and  $b$  are the low- and high-frequency power-law exponents of the  $\varepsilon''(\nu)$  minimum, as will be explained in detail in Sec. IV C 1. The solid line in Fig. 5(c) is a fit with the three-parameter function, Eq. (3), with  $\gamma = 2.72$  and  $T_c = 187$  K fixed to the values obtained from the analysis of the  $\varepsilon''(\nu)$  minimum (Sec. IV C 1). Even with all parameters free, very similar values result, namely  $T_c = 185$  K and  $\gamma = 2.78$ . For the fits, only data above 200 K were used where a good agreement between data and fit was achieved. The inset shows the same curves in a Stickel plot. In order to describe the data at lower temperatures, a VFT fit can be employed (dashed line in the inset and main frame). The change of slope, seen in the Stickel plot near 200 K [49], then marks the transition from VFT to MCT behavior. The observed absence of critical behavior at  $T_c$  in the experimental data is expected within the extended MCT [3,4]. Here the structural arrest found in idealized MCT for  $T < T_c$  is avoided by the assumption of thermally activated hopping processes. MCT also predicts that, at least for  $T > T_c$ , the relaxation times determined with different experimental methods should follow a common temperature behavior. Indeed, while there is a difference in the absolute values of  $\tau$  from light scattering [15] and dielectric measurements (leading to the different  $\alpha$ -peak positions in Fig. 4), which can be understood considering the different correlation functions of both methods [60], they can be transferred into each other by a temperature-independent factor of about 3 (not shown).

Finally, we compare the results to the predictions of the frustration-limited domain (FLD) model by Kivelson, Tarjus, and co-workers [7]. This theory postulates a ‘‘narrowly avoided critical point’’ at a temperature  $T^*$  above the melting point. The theory is based on the assumption that there is a locally preferred structure (LPS) which, however, is not able to tile space periodically. Without this geometrical constraint the system would condense into the LPS at  $T^*$ . In real systems somewhat below  $T^*$ , frustration-limited domains with the LPS are formed. Such a scenario is intuitive for the simple system of spherical molecules. Here the LPS is an icosahedral short-range order but one cannot tile space with this structure. By using a phenomenological scaling approach, a prediction for the temperature-dependent relaxation rate was obtained:

$$\nu_p = \nu_\infty \exp\left(-\frac{E_\infty}{T}\right) \quad \text{for } T > T^*, \quad (4)$$

$$\nu_p = \nu_\infty \exp\left[-\frac{E_\infty}{T} - \frac{FT^*}{T} \left(\frac{T^* - T}{T^*}\right)^{8/3}\right] \quad \text{for } T < T^*.$$

Good agreement of this four-parameter function with the results in a variety of glass formers was found [61]. This is also valid for the present results on PC as demonstrated in Fig. 5(d). However, in the Stickel plot (inset) the small deviations, seen at high temperatures, are more pronounced and the agreement between data and fit seems rather poor. The abrupt transition between two functional forms at  $T^*$  may be a reason for these difficulties, which possibly could be overcome by using a smoother transition.

Clearly, among the analyses presented in Fig. 5, the one employing the combination of VFT and thermally activated behavior [Fig. 5(a)] seems least reasonable as there is no theoretical base for such a behavior. As could be expected, the two four-parameter functions (EFV and FLD model) provide the best descriptions of the data as was also found for a similar comparison performed for dielectric results on Salol [12]. As mentioned above, the huge deviations seen for the (idealized) MCT approach could be expected. This setback may be overcome when employing the extended MCT, which is out of the scope of the present work. An argument in favor of the MCT fit is the fact that only one parameter was varied,  $T_c$  and  $\gamma$  being fixed as mentioned above.

The MCT also makes distinct predictions for the temperature dependence of the relaxation strength  $\Delta\varepsilon$  and the spectral form of the  $\alpha$  process [2–4]. According to idealized MCT, for  $T > T_c$ , the relaxation strength and the spectral form of the  $\alpha$  process should be temperature independent (time-temperature superposition principle). In addition, for  $T < T_c$ ,  $\Delta\varepsilon = c_1 + c_2[(T_c - T)/T_c]^{1/2}$  follows from extended MCT. In Fig. 3(a) the solid line was calculated using the MCT prediction with  $T_c = 187$  K as deduced in Sec. IV C 1. Due to the scattering of the data, no definite conclusion can be drawn, but at least the data do not contradict MCT. In contrast, Schönhalz *et al.* [43] reported clear deviations of their  $\Delta\varepsilon(T)$  (given in arbitrary units) from MCT predictions [62]. Concerning the predicted temperature-independent spectral form of the  $\alpha$  peak for  $T > T_c$ , a tendency to saturate is indeed seen for  $\beta_{CD}(T)$  and  $\beta_{KWW}(T)$  in Fig. 3, however

at temperatures clearly above  $T_c$  only. But a reasonable description of the  $\alpha$  peaks for  $T > T_c$  is also possible with a constant  $\beta_{CD} \approx 0.8$ . Again this is in contrast to the statements made in [43]. Overall it is difficult to make a decisive statement about the validity of MCT in PC from the analysis of the  $\alpha$  process alone.

### B. Excess wing

The excess wing (also called ‘‘high-frequency wing’’ or ‘‘tail’’) seems to be a universal feature of glass-forming liquids [8,63], but up to now its microscopic origin remains unclear. A phenomenological function taking account of the  $\alpha$  peak and the wing has been proposed recently [64]. In many cases it is possible to describe the  $\alpha$  peak including the wing using a model of dynamically correlated domains [6], but for low temperatures and extremely broadband data, deviations show up [65]. Also, the FLD model is able to describe the wing at least partly [7].

Nagel and co-workers [8] found that the  $\epsilon''(\nu)$  curves for different temperatures and even for different materials, including the  $\alpha$  peak and the wing, can be scaled onto one master curve by an appropriate choice of the  $x$  and  $y$  axis. This intriguing scaling behavior strongly suggests a correlation between the  $\alpha$  process and the high-frequency wing. However, until now there has been no theoretical justification for the choice of the plotted quantities. During recent years some criticism of the Nagel scaling arose concerning its universality [66,67] and accuracy [67,68] and minor modifications of the original scaling procedure have been proposed [67]. However, it is still commonly believed that the Nagel scaling is of significance for our understanding of the glass-forming liquids and many efforts have been made to check its validity in a variety of materials [47,66,68–70].

In Fig. 6 we have applied the modified scaling approach proposed by Dendzik *et al.* [67]. This procedure was shown to lead to somewhat better scaling in the  $\alpha$ -peak region and allows for an unequivocal determination of the scaling parameters. In addition, the modified procedure is able to collapse different CD curves onto one master curve [67], which is not the case for the original Nagel scaling [69]. As demonstrated in Fig. 2, the CD function gives an excellent description of the  $\alpha$ -peak region in  $\epsilon''(\nu)$ . The application of the modified scaling requires the determination of parameters  $\nu_s$ ,  $\epsilon_s''$ , and  $\beta$ . Here  $\nu_s$  and  $\epsilon_s''$  are defined as frequency and amplitude of the intersection point of the two power laws  $\epsilon'' \sim \nu$  for  $\nu < \nu_p$  and  $\epsilon'' \sim \nu^{-\beta}$  for  $\nu > \nu_p$ . In Fig. 6 we show the PC results in addition to glycerol data taken from [27], scaled according to [67], i.e., with  $x = (1 + \beta) \log_{10}(\nu/\nu_s)$  and  $y = \log_{10}[\epsilon'' \nu_s / (\epsilon_s'' \nu)]$ . Indeed, the  $\alpha$  peak and the excess wing region can be scaled nicely onto one master curve for each material. The deviations from this master curve seen in Fig. 6 occur in the minimum and boson peak region, which cannot be scaled in this way. The scaling transfers the CD behavior of the  $\alpha$  peak to a constant,  $y = 0$ , at its low-frequency side ( $x < 0$ ) and to a linear decrease,  $y = -x$  (solid lines in Fig. 6), at its high-frequency side ( $x > 0$ ). The excess wing shows up as a more shallow linear decrease deviating from the  $y = -x$  line above  $x \approx 5$ . Due to the large frequency region available for the present work this linear decrease can be observed up to  $x = 20$  for PC while the maximum value

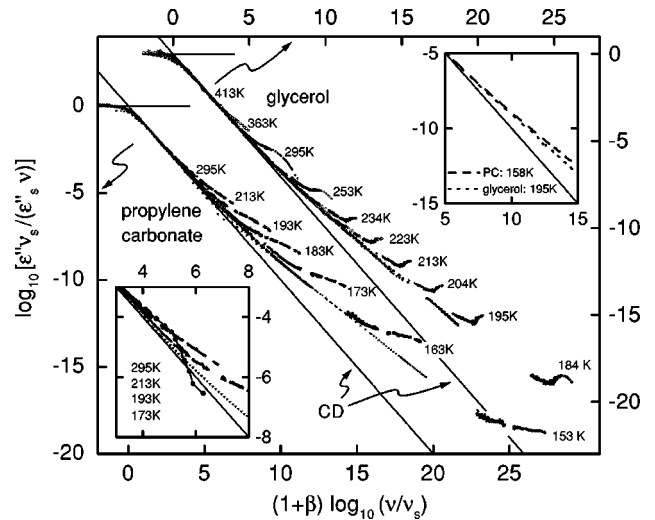


FIG. 6. Scaling plot of  $\epsilon''(\nu)$  for PC and glycerol according to [67].  $\nu_s$  and  $\epsilon_s''$  are read off at the intersection point of the two power laws  $\epsilon'' \sim \nu$  and  $\epsilon'' \sim \nu^{-\beta}$  below and above the peak frequency, respectively. Note that for clarity reasons both data sets are shifted with respect to each other. The lines show the asymptotic behavior for a CD function at  $\nu < \nu_p$  and  $\nu > \nu_p$ . The lower inset is a magnified plot for the transition region between CD and excess wing contribution in PC. Here the 295 K points are connected by a solid line to guide the eye. The upper inset shows one glycerol and one PC curve in the wing region.

observed up to now was  $x \approx 11$  [67]. Due to this larger range it becomes obvious that the curves for glycerol and PC show significant deviations from each other at  $x \geq 10$  as demonstrated in the upper inset of Fig. 6. In contrast, the original Nagel scaling [8] scales the curves for both materials much better in this high-frequency region [71]. As mentioned above, the wing seems to merge with the  $\alpha$  peak above about 200 K. In Fig. 6 this corresponds to a direct transition from  $y = -x$  behavior to the nonscaling linear decrease corresponding to the minimum region (see the lower inset of Fig. 6). Here only two linear regions for  $x > 0$  can be distinguished while at lower temperatures three such regions are seen (associated with the  $\alpha$  peak, excess wing, and minimum). For glycerol a similar merging of wing and  $\alpha$  peak is observed at temperatures above about 270 K.

Finally we want to mention that it is also possible to describe the excess wing by an additional relaxation process superimposed to the  $\alpha$  process [21]. Such secondary processes, usually termed (slow)  $\beta$  processes, can often be ascribed to an internal change of the molecular conformation. However, in the light of the universal properties of the wing for different glass-forming liquids revealed by the Nagel scaling, it is unreasonable to ascribe it to this type of  $\beta$  relaxations which depend on the specific molecular structure. The finding that secondary relaxation processes can show up also in simple glass formers led to the assumption of a more fundamental reason for these so-called Johari-Goldstein  $\beta$  processes [38]. Also recent theoretical developments [72] within the coupling model [5] may point in the direction of a universal slow  $\beta$  relaxation, closely connected to the  $\alpha$  process. It cannot be excluded that the wing and these possible intrinsic  $\beta$  relaxations are manifestations of the same microscopic mechanism.

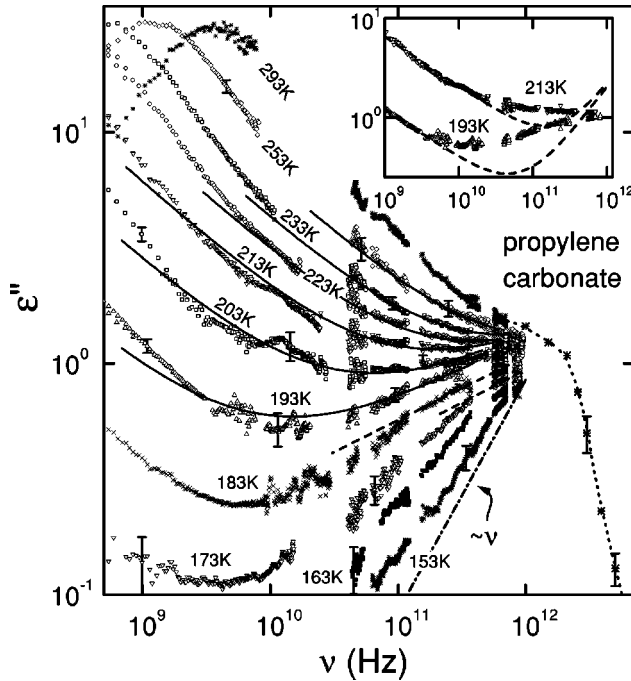


FIG. 7.  $\epsilon''(\nu)$  at high frequencies for various temperatures. The solid lines are fits with MCT, Eq. (7), with  $a=0.29$  and  $b=0.5$  ( $\lambda=0.78$ ). The dashed lines demonstrate  $\nu^a$  behavior for  $T < T_c$ . The dash-dotted line indicates linear behavior. The dotted line is drawn to guide the eye. The dashed lines in the inset have been calculated with Eq. (5).

### C. Fast dynamics

#### 1. $\epsilon''(\nu)$ minimum

In Fig. 7, a magnified view of the high-frequency region of  $\epsilon''(\nu)$  is shown. In the inset we try to analyze the minimum region in terms of a simple crossover from  $\alpha$  relaxation or excess wing to the boson peak. For the low-frequency wing of the boson peak a linear or steeper increase of  $\epsilon''(\nu)$  can be assumed as is commonly found for a variety of glass formers [11,12,73]. Indeed, for the lowest temperatures investigated, where vibrational contributions can be assumed to become dominant, a linear increase of  $\epsilon''(\nu)$  (dashed line in Fig. 7) is approached. Also, in order for the boson peak to appear in the light- or neutron-scattering spectra (where it was first observed),  $\epsilon'' \sim \nu S(q, \nu)$  must increase steeper than linearly towards the boson peak. The dashed lines in the inset of Fig. 7 have been calculated by a sum of two power laws,

$$\epsilon'' \sim c_b \nu^{-b} + c_n \nu^n, \quad (5)$$

with  $n=1$  [74].  $b$  was chosen to match the power law seen in  $\epsilon''(\nu)$  between 1 GHz and the  $\epsilon''(\nu)$  minimum. Clearly there is no way to obtain a reasonable fit of the experimental data in this way. This analysis clearly implies the presence of additional fast processes in this region, usually termed fast  $\beta$  processes. Similar findings were obtained for a variety of glass formers [12,18,19,47].

Fast processes are not considered in the EFV model [56,59], which provides the best fits to the dynamics of the  $\alpha$  process (Sec. IV A). Within this model, molecules are assumed to move within cages formed by their next neighbors and diffusional motion occurs by hopping into “free vol-

ume” available to the molecule. It is interesting that this picture is qualitatively similar to that of MCT, where fast processes are a natural consequence of the theory. But a theoretical investigation of these possible fast processes in the EFV is missing. In the FLD model [7] the  $\alpha$  relaxation is identified with the restructuring of the FLDs and occurs on a length scale given by their characteristic size. Within the FLD framework there is a second length scale, the correlation length  $\xi$  of the LPS. It was argued [7] that the experimentally observed fast  $\beta$  processes may be ascribed to fast relaxations taking place on this smaller length scale of the FLD model. However, up to now a theoretical elaboration of the fast processes within FLD theory was missing.

Another model predicting fast processes is the coupling model (CM) of Ngai and co-workers [5]. Here the fast process is part of the  $\alpha$  relaxation, defined in the time domain. The  $\alpha$  relaxation is assumed to be composed of a fast exponential decay with relaxation time  $\tau_f$  at short times  $t < t_c$ , and a slower KWW behavior with relaxation time  $\tau_s$  and stretching parameter  $\beta_s$  at  $t > t_c$ . The crossover time  $t_c$  was stated to be of the order of ps for most systems [5]. Demanding continuity at  $t_c$  leads to the relation

$$\tau_f = \tau_s^{\beta_s} t_c^{1-\beta_s}. \quad (6)$$

This allows for the determination of the relaxation time  $\tau_f$  of the fast process, if the KWW parameters of the slow process are known. The parameters determined from the KWW fits of the  $\alpha$  relaxation in PC (Sec. IV A) result in a factor  $\tau_s/\tau_f \approx 1.3$  for the highest temperature and  $\tau_s/\tau_f \approx 10^4$  for 153 K. Obviously, the fast process inherent in the CM is located at much lower frequencies than the  $\epsilon''(\nu)$  minimum and therefore cannot be brought into play for the explanation of the excess intensity in this region. Instead additional contributions need to be assumed but, as shown in the beginning of this section, a combination of  $\alpha$  process (even including the CM’s fast process) and boson peak alone cannot take account of the experimental data. Further contributions may arise [75], e.g., from a constant loss term as early proposed by Wong and Angell [24] and/or a possible  $\epsilon'' \sim \nu^{0.3}$  behavior, both seemingly universal features in the dielectric response of glassy ionic conductors [76,77]. Possible microscopic explanations for these contributions were proposed in [77]. Indeed, the data in PC near the  $\epsilon''(\nu)$  minimum can well be described by adding a term  $\epsilon_c + c_3 \nu^{0.3}$  to the ansatz of Eq. (5) [78]. In this way, by adjusting the parameters to achieve a smooth transition to the CD curves describing the  $\alpha$  peak, quite impressive fits over 17 decades of frequency are possible. Of course this could be expected considering the large amount of parameters involved in the fitting, but nevertheless it cannot be excluded that such a simple superposition ansatz of different independent contributions is correct.

Very recently a model was proposed considering a low-frequency relaxationlike part of the vibration susceptibility function responsible for the boson peak [79]. This relaxationlike response was shown to arise from anharmonicity of vibrations and invoked to explain the quasielastic line seen in light and neutron scattering. This quasielastic contribution corresponds to the fast  $\beta$  process seen in the region below the boson peak in the susceptibility spectra. Within this

framework, the fast process should show up as a peak with  $\varepsilon'' \sim \nu^\alpha$  and  $\varepsilon'' \sim \nu^{-1}$  at its low- and high-frequency side, respectively. For the absolute value of the exponent  $\alpha$ , reasonable values ranging between 0.375 and 1 were given in [79], depending on the system. Of course no peak is seen between  $\alpha$  and the boson peak in the spectra of PC (Figs. 2 and 7) but the  $\nu^{-1}$  wing of the fast  $\beta$  process may be obscured by the domination of the boson peak at higher frequencies. A severe argument against this picture is the smooth transition of  $\varepsilon''(\nu)$  from the minimum to the boson peak with only one power law, which seems unlikely to result from the superposition of the  $\nu^\alpha$  wing of the fast  $\beta$  process and the low-frequency wing of the boson peak (steeper than  $\nu^1$ , see above). However, this possibility cannot fully be excluded and at least this model provides an explanation for the sublinear increase seen for  $\nu > \nu_{\min}$ . It is interesting that within this theoretical framework a crossover temperature of the fast relaxation was obtained which was found to be of similar magnitude as the critical temperature  $T_c$  of MCT [79].

As mentioned in the Introduction, a fast process in the minimum region of  $\varepsilon''(\nu)$  is one of the main outcomes of MCT, a prediction which led to the tremendous interest in this high-frequency region. Within idealized MCT, above  $T_c$ , the high- and low-frequency wings close to the minimum of  $\varepsilon''(\nu)$  are described by power laws with exponents  $a$  and  $b$ , respectively. The minimum region can be approximated by the interpolation formula [2,3]:

$$\varepsilon''(\nu) = \varepsilon''_{\min} [a(\nu/\nu_{\min})^{-b} + b(\nu/\nu_{\min})^a] / (a+b). \quad (7)$$

$\nu_{\min}$  and  $\varepsilon''_{\min}$  denote position and amplitude of the minimum, respectively. The exponents  $a$  and  $b$  are temperature independent and constrained by the exponent parameter  $\lambda = \Gamma^2(1-a)/\Gamma(1-2a) = \Gamma^2(1+b)/\Gamma(1+2b)$ , where  $\Gamma$  denotes the Gamma function. This restricts the exponent  $a$  to values below 0.4, i.e., a significantly sublinear increase of  $\varepsilon''(\nu)$  at frequencies above the minimum is predicted. We found a consistent description of the  $\varepsilon''$  minima at  $T \geq 193$  K using  $\lambda = 0.78$ , which implies  $a = 0.29$  and  $b = 0.5$  (solid lines in Fig. 7). The obtained  $\lambda$  agrees with that determined from the preliminary data published previously [19,25,26]. It is identical to  $\lambda$  deduced from light-scattering results [15] and also consistent with a recent analysis of solvation dynamics experiments on PC [80]. In addition, a preliminary analysis of the susceptibility minimum from recent neutron-scattering measurements [54] yields  $\lambda = 0.75$ , consistent with the present value. At high frequencies the fits with Eq. (7) are limited by the onset of the decrease at the high-frequency wing of the boson peak. Quite a different behavior was seen in glycerol [26,78], where the MCT fits are limited at high frequencies by an additional increase, which cannot be described by Eq. (7). In [26,78] it was argued that this deviation in glycerol is due to the vibrational boson peak contribution which is not taken into account by Eq. (7). In PC this contribution seems to be of less importance. This is in accord with the finding of Sokolov *et al.* [32] that the amplitude ratio of boson peak and fast process is largest for strong glass formers, glycerol being much stronger than PC (see also Sec. IV C 3). The deviations of data and fits, seen at low frequencies in Fig. 7, can be ascribed to the growing importance of

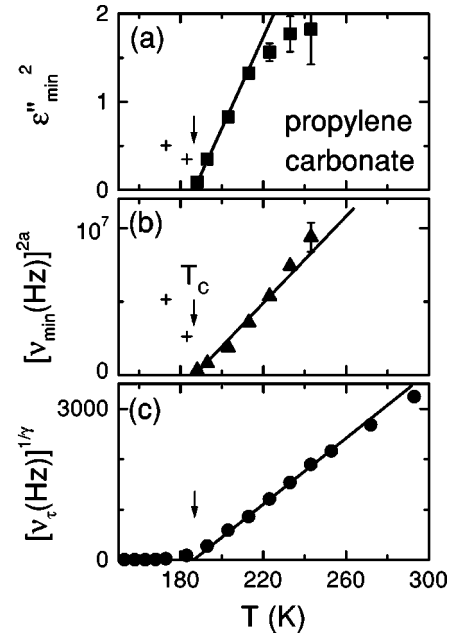


FIG. 8. Temperature dependence of the amplitude (a) and position (b) of the  $\varepsilon''(\nu)$  minimum and of the  $\alpha$ -peak position  $\nu_\tau = 1/(2\pi(\tau)_{\text{CD}})$  (c) of PC.  $\varepsilon''_{\min}$  and  $\nu_{\min}$  have been taken from the fits with Eq. (7). Representations have been chosen that result in straight lines according to the predictions of the MCT. The solid lines extrapolate to a  $T_c$  of 187 K for all three quantities as indicated by the arrows. The pluses give an estimate for the position of the tentative “knee,” which may be suspected from Fig. 7.

the  $\alpha$  relaxation, which is not taken into account by the simple interpolation formula, Eq. (7).

The critical temperature  $T_c$  should manifest itself in the temperature dependence of the  $\varepsilon''(\nu)$  minimum. For  $T > T_c$ , MCT predicts the following relations:  $\nu_{\min} \sim (T - T_c)^{1/(2a)}$  and  $\varepsilon''_{\min} \sim (T - T_c)^{1/2}$ . Figure 8 shows the results for  $\varepsilon''_{\min}(T)$ ,  $\nu_{\min}(T)$ , and also for  $\nu_\tau(T)$  (same data as in Fig. 5). Here representations have been chosen that lead to straight lines that extrapolate to  $T_c$  if the predicted critical temperature dependences are obeyed. Indeed, as indicated by the solid lines, all three data sets can be described consistently with a critical temperature  $T_c \approx 187$  K, in agreement with the results determined from the preliminary data published previously [19,25,26]. This lies in the same range as the  $T_c$  obtained from light scattering [15] (187 K), neutron scattering [81] (180–200 K), and solvation dynamics experiments [80] (176 K). Also the  $T_c \approx 186$  K, deduced from a preliminary analysis of the susceptibility minimum from recent neutron-scattering experiments [54], agrees well with the present value. For temperatures near  $T_c$ , the  $\nu_\tau$  data deviate from the predicted behavior as also seen in Fig. 5(c). Within MCT this can be ascribed to a smearing out of the critical behavior near  $T_c$  due to hopping processes which are considered in extended versions of MCT only [3,4]. In addition, the above critical temperature dependences of  $\varepsilon''_{\min}$ ,  $\nu_{\min}$ , and  $\nu_p$  should be valid only for temperatures not too far above  $T_c$  and the deviations seen for  $\nu_{\min}$  and  $\varepsilon''_{\min}$  at high temperatures (Fig. 8) may be due to this fact. Therefore, there is a problem concerning the proper choice of the temperature range to be used for the determination of  $T_c$ . While the critical behavior proposed in Fig. 8 seems reasonable, some

uncertainties concerning the value of  $T_c$  remain, which can only be clarified by an analysis within the extended MCT [82].

MCT predicts a significant change in the behavior of  $\varepsilon''(\nu)$  at  $T_c$ : For  $T < T_c$ , within idealized MCT  $\varepsilon''(\nu)$  should exhibit a so-called “knee” at a frequency  $\nu_k$ , i.e., a change of power law from  $\varepsilon'' \sim \nu^a$  at  $\nu > \nu_k$  to  $\varepsilon'' \sim \nu$  at  $\nu < \nu_k$ . Within idealized MCT, at  $T < T_c$  the minimum and the  $\alpha$  peak should vanish but both phenomena are restored by the hopping processes invoked in extended MCT [3,4]. At first, from Fig. 7 it becomes obvious that the fits with Eq. (7) with  $\lambda = 0.78$  will no longer work at  $T < T_c$  because the high-frequency wing of the minimum becomes successively steeper below this temperature, i.e., the frequency dependence of  $\varepsilon''(\nu)$  changes significantly below  $T_c$ . In Fig. 7, an  $\varepsilon'' \sim \nu^a$  behavior with  $a = 0.29$  as determined for  $T > T_c$  is shown as a dashed line matching the region just below the boson peak for the 183 K and 173 K curves. For lower frequencies the experimental data exhibit a downward deviation from the  $\nu^a$  extrapolations, i.e., really a knee appears. Nevertheless, in light of the rather large experimental uncertainties in this region it seems quite audacious to assign the observed feature to the knee of MCT. According to MCT,  $\nu_k$  and the amplitude at the knee,  $\varepsilon_k''$ , should also exhibit critical behavior,  $\nu_k \sim (T_c - T)^{1/(2a)}$  and  $\varepsilon_k'' \sim (T_c - T)^{1/2}$ , with the proportionality factors in close connection with the proportionality factors in the critical behavior of the minimum [83]. In Figs. 8(a) and 8(b) the two values read off from Fig. 7 are denoted as pluses. Having in mind the extreme uncertainties in the knee position, the data seem to be consistent with a  $T_c$  of 187 K. However, the position of the knee is not in accord with the position of the minimum above  $T_c$  [83]. Overall, a lack of significance of the observed knee feature has to be stated but at least the data show where the knee may be located and where more experimental work has to be done to check for its presence and temperature evolution in PC.

## 2. Comparison with scattering results

The comparison of dielectric and scattering results is shown in Fig. 4. As mentioned above (Sec. III B), the significantly larger ratio of  $\alpha$  and the boson peak amplitude for dielectric compared with light-scattering results seems to be a rather universal property of glass-forming materials [26,27,52,53]. Recently, an explanation for this finding was given by considering the different dependencies of the probes on orientational fluctuations [84]. In addition, in a recent theoretical work [85], MCT was generalized to molecular liquids of molecules with orientational degrees of freedom. The resulting MCT equations were solved for a system of dipolar hard spheres and a larger ratio of  $\alpha$  and the boson peak amplitude for  $\varepsilon''$  was obtained in accordance with the experimental findings. Furthermore, it is one of the main predictions of MCT [2–4] that the same parameters  $T_c$  and  $\lambda$  should arise from all observables coupling to the density fluctuations. This is indeed the case for propylene carbonate (see above). But also the position of the  $\varepsilon''$  (respectively  $\chi''$ ) minima should be the same, independent of the experimental method, which is also valid when including orientational degrees of freedom [60]. However, as seen in Fig. 4, this seems not to be the case. An explanation for a

similar behavior found from molecular-dynamics simulations of a system of rigid diatomic molecules was given in terms of 180° flips of the nonspherical molecules, which cannot be taken into account by a hard-sphere model [53]. In this context, it may be mentioned that for the mobile-ion glass-former KKN a rather good agreement of the minimum position from different experimental methods was found [25]. Here orientational degrees of freedom are not important, which corroborates the above explanation in terms of 180° flips.

## 3. Boson peak

The boson peak is a universal feature of glass-forming materials showing up in light and neutron scattering but also as excess contribution in specific-heat measurements. A variety of explanations of the boson peak has been proposed, e.g., in terms of the soft potential model [86], phonon localization models [87], or a model of coupled harmonic oscillators with a distribution of force constants [88]. Also MCT includes contributions leading to a peak at THz as was shown using a schematic two-correlator model [89]. However, up to now there is no consensus concerning the microscopic origin of this phenomenon. It cannot be the aim of the present paper to compare the results with the proposed models, especially in the light of the rather restricted database for  $\nu > 1$  THz. However, some experimental facts deserve to be emphasized which may be of importance for the understanding of the boson peak. Figure 9 shows the high-frequency region of  $\varepsilon''(\nu)$  for PC and glycerol. Clearly, both materials exhibit quite different behavior in the boson peak region: For PC only one power law is seen at frequencies  $\nu > \nu_{\min}$  forming simultaneously the high-frequency wing of the  $\varepsilon''$  minimum and the low-frequency wing of the boson peak. In marked contrast, for glycerol two regimes can be distinguished: Directly above  $\nu_{\min}$ , there is a rather shallow increase of  $\varepsilon''(\nu)$  which together with the left wing of the minimum can be well fitted with the MCT prediction, Eq. (7) [18,26,78]. At higher frequencies a very steep increase appears, approaching  $\varepsilon'' \sim \nu^3$  for  $T \rightarrow T_g$ . This different behavior of PC and glycerol also becomes obvious in the scaling plot of Fig. 6. For both materials the  $\varepsilon''(\nu)$  minimum corresponds to the deviation from the master curve, which shows up as a third linear region in the scaling plot. But for glycerol in addition a minimum is seen in Fig. 6. In the scaling plot this minimum marks the transition point between the two regimes at  $\nu > \nu_{\min}$ , described above. It seems that in glycerol the fast  $\beta$  process giving rise to the shallow minimum in  $\varepsilon''(\nu)$  or the third linear region in the scaling plot is obscured at higher frequencies by the boson peak contribution. This arguing seems to be in accord with the finding of Sokolov *et al.* [32] of a higher amplitude ratio of boson peak and fast process for strong glass formers. However, at least near  $T_g$  this ratio, e.g., measured by comparing boson peak and minimum amplitude in Fig. 9, is quite similar for both materials. For high temperatures,  $T \geq 193$  K for PC and  $T \geq 253$  K for glycerol, the fast  $\beta$  process in PC has indeed a higher amplitude if curves with similar values of  $\nu_p$  are compared. This fact also explains the good fits with MCT up to the boson peak frequency (Sec. IV C 1) in PC. However, for lower temperatures the different characteristics of PC and glycerol has to be ascribed either to a more shallow left wing

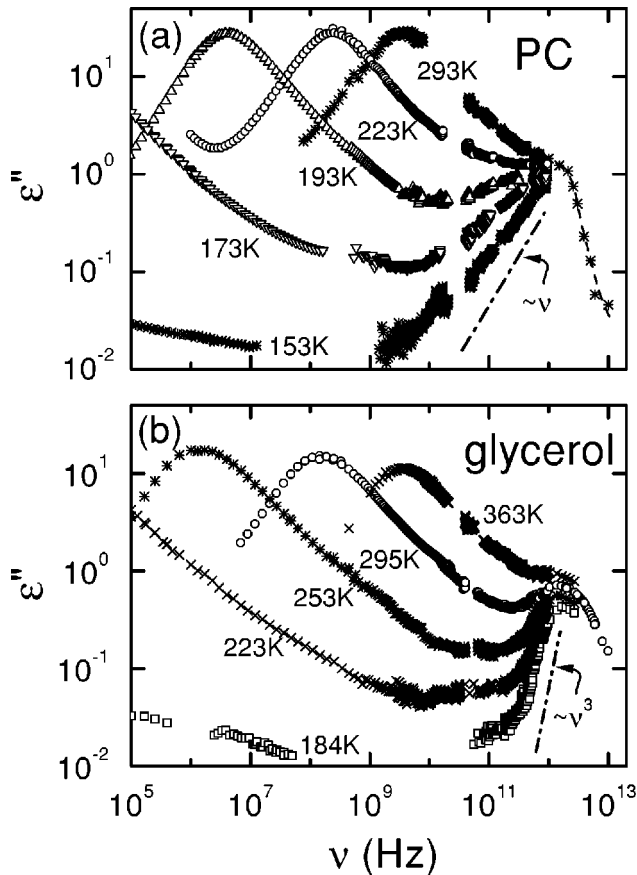


FIG. 9.  $\varepsilon''(\nu)$  in the high-frequency region for PC (a) and glycerol (b). The dash-dotted lines indicate power laws as noted in the figure. The dashed line in (a) was drawn to guide the eye.

of the boson peak for PC ( $\varepsilon'' \sim \nu^1$  instead of  $\varepsilon'' \sim \nu^3$ ) or to a steeper increase of the high-frequency wing of the minimum, thereby obscuring the steeper boson peak wing. Interestingly, while there might be some problems for the new model by Novikov [79] in explaining the PC results (see Sec. IV C 1), glycerol seems to fit into this picture: Below the boson peak, two distinct regions are seen which can be ascribed to the relaxationlike and the main part of the vibrational excitations. Concerning MCT, it has to be mentioned that the light-scattering results on glycerol [14] exhibit quite similar characteristics to the dielectric results [27]. The light-scattering results were successfully described using the schematic two-correlator MCT model mentioned above [89]. But it is not clear if MCT is able to provide an explanation for the qualitative difference of the glycerol and PC dielectric data.

#### D. Conclusions

Dielectric data on glass-forming PC in an exceptionally broad frequency range have been presented and compared with the results from light scattering and with broadband dielectric results on glycerol. A comparison of the findings concerning  $\alpha$  relaxation, excess wing,  $\varepsilon''(\nu)$  minimum, and boson peak on various theoretical and phenomenological predictions has been performed. The temperature dependence of the  $\alpha$ -relaxation time is in accord with the EFV and the FLD models and at high temperatures also with that of idealized MCT. The temperature dependences of the relax-

ation strength and the width parameter of the  $\alpha$  relaxation were determined and some differences from the findings from previous works were found. The excess wing in PC was shown to follow the modified Nagel scaling proposed by Dendzik *et al.* [67] but at high frequencies the curves of PC and glycerol do not scale onto each other. Overall, it is not possible to arrive at a decision in favor of or against one of the models on the dynamics of glass-forming materials from the results obtained at the first 15 decades of frequency alone.

At higher frequencies above about 1 GHz a minimum in  $\varepsilon''(\nu)$  is detected. In this region, clearly fast processes contribute to the dielectric loss, a finding for which most models provide no explanation. While the minimum can be well described by the sum of power laws and a constant loss contribution [78], the theoretical foundation for these contributions is unclear at present but currently is being developed [75]. In contrast, MCT provides a microscopic explanation for the high-frequency data, at least at high temperatures. In addition, the analysis within MCT yields values for  $T_c$  and  $\lambda$ , that are in agreement with those determined from other experimental methods. Also the differences in the susceptibilities obtained from dielectric and light scattering experiments seem to be in accord with recent extensions of MCT. At low temperatures,  $T < T_c$ , at least a qualitative agreement of the results with MCT can be stated, but more work is needed for a quantitative comparison [82].

Overall, certain aspects of the results found in the present work can be explained by different models, but in our judgment MCT provides the most consistent picture providing explanations for the largest variety of experimental facts, including the high-frequency processes. This may be partly due to the large amount of predictions made by MCT, covering almost all aspects of the dynamic response of glass-forming materials, while other models are somewhat restricted in this respect. However, just this agreement of the data with the many different predictions of MCT speaks in favor of the theory. Admittedly, it is not possible to arrive at a final decisive conclusion concerning the applicability of MCT for PC and alternative explanations may be possible. Also many questions need to be solved, e.g., the behavior below  $T_c$  should be compared with the extended MCT, the differences from the scattering results should be compared quantitatively to MCT (considering orientational degrees of freedom of dipolar, nonspherical molecules), and the qualitatively different behavior of PC and glycerol in the boson peak region should be addressed. Finally, in the boson peak region we find significant differences between glycerol and PC that still require a theoretical explanation. But also more experimental work is needed, e.g., concerning the temperature evolution of the boson peak and a higher precision of the data at low temperatures in order to investigate in detail the possible occurrence of a knee in  $\varepsilon''(\nu)$  of PC.

#### ACKNOWLEDGMENTS

We gratefully acknowledge stimulating discussions with C.A. Angell, R. Böhmer, H.Z. Cummins, W. Götze, K.L. Ngai, M. Ohl, R. Schilling, W. Schirmacher, and J. Wuttke. We thank M. Ohl and J. Wuttke for information on the re-

sults of the neutron scattering experiments of Ref. [54] prior to publication. We are grateful to H.Z. Cummins for providing the light scattering results shown in Fig. 4. We thank M. Dressel for assistance in the quasioptical measurements, and

Th. Wiedenmann for technical support. This work was supported by the Deutsche Forschungsgemeinschaft under Grant No. LO264/8-1, and partially by the BMBF under Contract No. 13N6917.

- 
- [1] See, e.g., M. Cable, in *Glasses and Amorphous Materials*, edited by J. Zarzycki, Materials Science and Technology, Vol. 9 (VCH, Weinheim, 1991), p. 1.
- [2] U. Bengtzelius, W. Götze, and A. Sjölander, *J. Phys. C* **17**, 5915 (1984); E. Leutheuser, *Phys. Rev. A* **29**, 2765 (1984); W. Götze, *Z. Phys. B* **60**, 195 (1985).
- [3] For a review of MCT, see W. Götze and L. Sjögren, *Rep. Prog. Phys.* **55**, 241 (1992).
- [4] W. Götze and L. Sjögren, *Z. Phys. B* **65**, 415 (1987).
- [5] K. L. Ngai, *Solid State Phys.* **9**, 127 (1979); K. L. Ngai, C. H. Wang, G. Fytas, D. L. Plazek, and D. J. Plazek, *J. Chem. Phys.* **86**, 4768 (1987).
- [6] R. V. Chamberlin, *Phys. Rev. B* **48**, 15 638 (1993).
- [7] D. Kivelson, S. A. Kivelson, X-L. Zhao, Z. Nussinov, and G. Tarjus, *Physica A* **219**, 27 (1995); G. Tarjus, D. Kivelson, and S. Kivelson, in *Supercooled Liquids: Advances and Novel Applications*, edited by J. T. Fourkas, D. Kivelson, U. Mohanty, and K. A. Nelson (ACS Publications, Washington, DC, 1997), p. 67.
- [8] P. K. Dixon, L. Wu, S. R. Nagel, B. D. Williams, and J. P. Carini, *Phys. Rev. Lett.* **65**, 1108 (1990).
- [9] N. Menon and S. R. Nagel, *Phys. Rev. Lett.* **74**, 1230 (1995).
- [10] See the collection of papers in *Disorder Effects on Relaxational Processes*, edited by R. Richert and A. Blumen (Springer, Berlin, 1994).
- [11] For a review of neutron scattering results, see W. Petry and J. Wuttke, *Transp. Theory Stat. Phys.* **24**, 1075 (1995).
- [12] H. Z. Cummins, G. Li, Y. H. Hwang, G. Q. Shen, W. M. Du, J. Hernandez, and N. J. Tao, *Z. Phys. B* **103**, 501 (1997).
- [13] See the collection of papers in *Dynamics of Glass Transition and Related Topics*, edited by T. Odagaki, Y. Hiwatari, and J. Matsui [*Prog. Theor. Phys. Suppl.* **126** (1997)]; *Structure and Dynamics of Glasses and Glass Formers*, edited by C. A. Angell, K. L. Ngai, J. Kieffer, T. Egami, and G. U. Nienhaus, Materials Research Society Symposium Proceedings No. 455 (MRS, Pittsburgh, 1997).
- [14] J. Wuttke, J. Hernandez, G. Li, G. Coddens, H. Z. Cummins, F. Fujara, W. Petry, and H. Sillescu, *Phys. Rev. Lett.* **72**, 3052 (1994); J. Wuttke, W. Petry, G. Coddens, and F. Fujara, *Phys. Rev. E* **52**, 4026 (1995).
- [15] W. M. Du, G. Li, H. Z. Cummins, M. Fuchs, J. Toulouse, and L. A. Knauss, *Phys. Rev. E* **49**, 2192 (1994).
- [16] A. Pimenov, P. Lunkenheimer, H. Rall, R. Kohlhaas, A. Loidl, and R. Böhmer, *Phys. Rev. E* **54**, 676 (1996).
- [17] K. L. Ngai, C. Cramer, T. Saatkamp, and K. Funke, in *Proceedings of the Workshop on Non-Equilibrium Phenomena in Supercooled Fluids, Glasses, and Amorphous Materials*, edited by M. Giordano, D. Leporini, and M. Tosi (World Scientific, Singapore, 1996), p. 3.
- [18] P. Lunkenheimer, A. Pimenov, M. Dressel, Yu. G. Goncharov, R. Böhmer, and A. Loidl, *Phys. Rev. Lett.* **77**, 318 (1996).
- [19] P. Lunkenheimer, A. Pimenov, M. Dressel, B. Gorshunov, U. Schneider, B. Schiener, and A. Loidl, in *Supercooled Liquids: Advances and Novel Applications*, edited by J. T. Fourkas, D. Kivelson, U. Mohanty, and K. A. Nelson (ACS Publications, Washington, DC, 1997), p. 168.
- [20] P. Lunkenheimer, A. Pimenov, and A. Loidl, *Phys. Rev. Lett.* **78**, 2995 (1997).
- [21] A. Hofmann, F. Kremer, E. W. Fischer, and A. Schönhals, in *Disorder Effects on Relaxational Processes*, edited by R. Richert and A. Blumen (Springer, Berlin, 1994), p. 309.
- [22] R. Brand, P. Lunkenheimer, U. Schneider, and A. Loidl, *Phys. Rev. Lett.* **82**, 1951 (1999).
- [23] D. W. Davidson and R. H. Cole, *J. Chem. Phys.* **19**, 1484 (1951).
- [24] J. Wong and C. A. Angell, in *Glass: Structure by Spectroscopy* (M. Dekker Inc., New York, Basel, 1974), p. 750.
- [25] P. Lunkenheimer, A. Pimenov, M. Dressel, B. Schiener, U. Schneider, and A. Loidl, *Prog. Theor. Phys. Suppl.* **126**, 123 (1997).
- [26] P. Lunkenheimer, A. Pimenov, M. Dressel, B. Gorshunov, U. Schneider, B. Schiener, R. Böhmer, and A. Loidl, in *Structure and Dynamics of Glasses and Glass Formers*, edited by C. A. Angell, K. L. Ngai, J. Kieffer, T. Egami, and G. U. Nienhaus, Materials Research Society Symposium Proceedings No. 455 (MRS, Pittsburgh, 1997), p. 47.
- [27] U. Schneider, P. Lunkenheimer, R. Brand, and A. Loidl, *J. Non-Cryst. Solids* **235-237**, 173 (1998).
- [28] C. A. Angell, in *Relaxations in Complex Systems*, edited by K. L. Ngai and G. B. Wright (NRL, Washington, DC, 1985), p. 3.
- [29] D. J. Plazek and K. L. Ngai, *Macromolecules* **24**, 1222 (1991); R. Böhmer and C. A. Angell, *Phys. Rev. B* **45**, 10 091 (1992).
- [30] A. Pimenov, P. Lunkenheimer, M. Nicklas, R. Böhmer, A. Loidl, and C. A. Angell, *J. Non-Cryst. Solids* **220**, 93 (1997).
- [31] R. Böhmer, K. L. Ngai, C. A. Angell, and D. J. Plazek, *J. Chem. Phys.* **99**, 4201 (1993).
- [32] A. P. Sokolov, E. Rössler, A. Kisliuk, and D. Quitmann, *Phys. Rev. Lett.* **71**, 2062 (1993).
- [33] F. I. Mopsik, *Rev. Sci. Instrum.* **55**, 79 (1984).
- [34] R. Böhmer, M. Maglione, P. Lunkenheimer, and A. Loidl, *J. Appl. Phys.* **65**, 901 (1989).
- [35] A. A. Volkov, Yu. G. Goncharov, G. V. Kozlov, S. P. Lebedev, and A. M. Prokhorov, *Infrared Phys.* **25**, 369 (1985); A. A. Volkov, G. V. Kozlov, S. P. Lebedev, and A. M. Prokhorov, *ibid.* **29**, 747 (1989).
- [36] M. Born and E. Wolf, *Principles of Optics* (Pergamon Press, Oxford, 1980).
- [37] C. A. Angell, L. Boehm, M. Oguni, and D. L. Smith, *J. Mol. Liq.* **56**, 275 (1993).
- [38] G. P. Johari and M. Goldstein, *J. Chem. Phys.* **53**, 2372 (1970).
- [39] R. Payne and I. E. Theodorou, *J. Phys. Chem.* **76**, 2892 (1972).
- [40] A. K. M. Masood, R. A. Pethrik, A. J. Barlow, M. G. Kim, R.

- P. Plowiec, D. Barraclough, and J. A. Ladd, *Adv. Mol. Relax. Processes* **9**, 29 (1976).
- [41] J. R. Huck, G. A. Noyel, L. J. Jorat, and A. M. Bondeau, *J. Electrostat.* **12**, 221 (1982).
- [42] J. Barthel, K. Bachhuber, E. Buchner, J. B. Gill, and M. Kleebauer, *Chem. Phys. Lett.* **167**, 62 (1990).
- [43] A. Schönhals, F. Kremer, A. Hofmann, E. W. Fischer, and E. Schlosser, *Phys. Rev. Lett.* **70**, 3459 (1993); A. Schönhals, F. Kremer, A. Hofmann, and E. W. Fischer, *Physica A* **201**, 263 (1993).
- [44] R. Böhmer, B. Schiener, J. Hemberger, and R. V. Chamberlin, *Z. Phys. B* **99**, 91 (1995).
- [45] R. L. Leheny and S. R. Nagel, *Europhys. Lett.* **39**, 447 (1997).
- [46] R. Kohlrausch, *Ann. Phys. (Leipzig)* **167**, 179 (1854); G. Williams and D. C. Watts, *Trans. Faraday Soc.* **66**, 80 (1970).
- [47] R. Brand, P. Lunkenheimer, and A. Loidl, *Phys. Rev. B* **56**, R5713 (1997).
- [48] C. J. F. Böttcher and P. Bordewijk, *Theory of Electric Polarization* (Elsevier, Amsterdam, 1978), Vol. II.
- [49] F. Stickel, E. W. Fischer, and R. Richert, *J. Chem. Phys.* **104**, 2043 (1996).
- [50] H. Vogel, *Z. Phys.* **22**, 645 (1921); G. S. Fulcher, *J. Am. Ceram. Soc.* **8**, 339 (1925); G. Tammann and W. Hesse, *Z. Anorg. Allg. Chem.* **156**, 245 (1926).
- [51] P. Lunkenheimer, R. Brand, U. Schneider, and A. Loidl, in *Slow Dynamics in Complex Systems: Eighth Tohwa University International Symposium*, AIP Conf. Proc. No. 469, edited by M. Tokuyama and I. Oppenheim (AIP, New York, 1999).
- [52] G. Wahnströhm and L. J. Lewis, *Prog. Theor. Phys. Suppl.* **126**, 261 (1997).
- [53] S. Kämmerer, W. Kob, and R. Schilling, *Phys. Rev. E* **58**, 2141 (1998).
- [54] J. Wuttke *et al.* (unpublished).
- [55] G. Adam and J. H. Gibbs, *J. Chem. Phys.* **43**, 139 (1965).
- [56] M. H. Cohen and D. Turnbull, *J. Chem. Phys.* **31**, 1164 (1959).
- [57] H. Z. Cummins, J. Hernandez, W. M. Du, and G. Li, *Phys. Rev. Lett.* **73**, 2935 (1994).
- [58] F. Stickel, E. W. Fischer, and R. Richert, *J. Chem. Phys.* **102**, 6251 (1995).
- [59] M. H. Cohen and G. S. Grest, *Phys. Rev. B* **20**, 1077 (1979); G. S. Grest and M. H. Cohen, *Adv. Chem. Phys.* **48**, 455 (1981).
- [60] R. Schilling (private communication).
- [61] D. Kivelson, G. Tarjus, X. Zhao, and S. A. Kivelson, *Phys. Rev. E* **53**, 751 (1996).
- [62] These authors compared  $T\Delta\epsilon(T)$  with MCT, presumably in order to correct for dipolar interactions dominating their  $\Delta\epsilon(T)$ , in contrast to the findings in the present work.
- [63] In a recent investigation [22] we have shown that the excess wing is not universally present in *orientationally* disordered materials, i.e., it seems to be a property inherent to *structural* glass formers.
- [64] A. Kudlik, Ph.D. thesis, Universität Bayreuth, 1997.
- [65] However, a recent extension of the model may enable a description of the complete spectra even including the minimum region [R. V. Chamberlin, *Phys. Rev. Lett.* **82**, 2522 (1999)].
- [66] A. Schönhals, F. Kremer, and E. Schlosser, *Phys. Rev. Lett.* **67**, 999 (1991).
- [67] Z. Dendzik, M. Paluch, Z. Gburski, and J. Ziolo, *J. Phys.: Condens. Matter* **9**, L339 (1997).
- [68] A. Kudlik, S. Benkhof, R. Lenk, and E. Rössler, *Europhys. Lett.* **32**, 511 (1995).
- [69] N. Menon, K. P. O'Brien, P. K. Dixon, L. Wu, S. R. Nagel, B. D. Williams, and J. P. Carini, *J. Non-Cryst. Solids* **141**, 61 (1992).
- [70] D. L. Leslie-Pelecky and N. O. Birge, *Phys. Rev. Lett.* **72**, 1232 (1994).
- [71] U. Schneider, R. Brand, P. Lunkenheimer, and A. Loidl (unpublished).
- [72] K. L. Ngai, *Phys. Rev. E* **57**, 7346 (1998); K. L. Ngai (private communication).
- [73] U. Strom, J. R. Hendrickson, R. J. Wagner, and P. C. Taylor, *Solid State Commun.* **15**, 1871 (1974); U. Strom and P. C. Taylor, *Phys. Rev. B* **16**, 5512 (1977); C. Liu and C. A. Angell, *J. Chem. Phys.* **93**, 7378 (1990).
- [74] One has to be aware that the assumption of an additive superposition of different contributions to the susceptibility may be oversimplified [for an alternative see, e.g., J. Colmenero, A. Arbe, and A. Alegria, *Phys. Rev. Lett.* **71**, 2603 (1993)] but at least it seems sufficient for a preliminary analysis.
- [75] K. L. Ngai (private communication).
- [76] W. K. Lee, H. F. Liu, and A. S. Nowick, *Phys. Rev. Lett.* **67**, 1559 (1991); D. L. Sidebottom, P. F. Green, and R. K. Brow, *ibid.* **74**, 5068 (1995); C. Cramer, K. Funke, and T. Saatkamp, *Philos. Mag. B* **71**, 701 (1995).
- [77] R. H. Cole and E. Tombari, *J. Non-Cryst. Solids* **131-133**, 969 (1991); K. L. Ngai, U. Strom, and O. Kanert, *Phys. Chem. Glasses* **33**, 109 (1992); B. S. Lim, A. V. Vaysleyb, and A. S. Nowick, *Appl. Phys. A: Solids Surf.* **56**, 8 (1993); S. R. Elliott, *Solid State Ionics* **70/71**, 27 (1994); D. L. Sidebottom, P. F. Green, and R. K. Brow, *J. Non-Cryst. Solids* **203**, 300 (1996); K. L. Ngai, H. Jain, and O. Kanert, *ibid.* **222**, 383 (1997).
- [78] P. Lunkenheimer, U. Schneider, R. Brand, and A. Loidl, in *Slow Dynamics in Complex Systems: Eighth Tohwa University International Symposium* (Ref. [51]), p. 433.
- [79] V. N. Novikov, *Phys. Rev. B* **58**, 8367 (1998).
- [80] J. Ma, D. Vanden Bout, and M. Berg, *Phys. Rev. E* **54**, 2786 (1996).
- [81] L. Börjesson, M. Elmroth, and L. M. Torell, *Chem. Phys.* **149**, 209 (1990).
- [82] Indeed, a very recent analysis of the present results using a schematic two-correlator model within the framework of extended MCT led to a good description of the data with  $T_c = 179$  K [W. Götze and T. Voigtmann (private communication)].
- [83] W. Götze (private communication).
- [84] M. J. Lebon, C. Dreyfus, Y. Guissani, R. M. Pick, and H. Z. Cummins, *Z. Phys. B* **103**, 433 (1997).
- [85] R. Schilling and T. Scheidsteiger, *Phys. Rev. E* **56**, 2932 (1997).
- [86] V. G. Karpov, M. I. Klinger, and F. N. Ignatiev, *Zh. Éksp. Teor. Fiz.* **84**, 760 (1983) [*Sov. Phys. JETP* **57**, 439 (1983)]; U. Buchenau, Yu. M. Galperin, V. L. Gurevich, D. A. Parshin, M. A. Ramos, and H. R. Schober, *Phys. Rev. B* **46**, 2798 (1992).
- [87] V. K. Malinovsky, V. N. Novikov, and A. P. Sokolov, *J. Non-Cryst. Solids* **90**, 485 (1987); S. R. Elliott, *Europhys. Lett.* **19**, 201 (1992).
- [88] W. Schirmacher, G. Diezemann, and C. Ganter, *Phys. Rev. Lett.* **81**, 136 (1998).
- [89] T. Franosch, W. Götze, M. R. Mayr, and A. P. Singh, *Phys. Rev. E* **55**, 3183 (1997).